

Scalar and conformal Holographic Artificial Impedance Surface Antennas

Jun Ouyang*, Yuan Zhang, Yu Long, Feng Yang, Jun Hu

* School of Electronic Engineering, University of Electronic Science and Technology of China, Chengdu 611731, Sichuan, China. Email: antenna_ou@163.com

Abstract

Three different kinds of artificial holographic impedance surface antennas are presented in this paper. The split main lobe problem of a plane surface is analyzed and overcome by introducing surface current theory. Both a conical conformal antenna and a cylindrical conformal antenna are designed to demonstrate the conformal capacities of these antennas. A spiral circularly polarized antenna is also proposed for the first time. All the analyses and simulation results have shown great prospects of artificial holographic impedance surface antennas.

1. Introduction

By combining the principle of surface impedance modulation with microwave holography, impedance surfaces that generate directive radiation patterns are theoretically designed [1-3]. In this paper, the new way of impedance modulation is proposed for the first time. We have implemented holographic antennas using modulated artificial impedance surfaces built as printed metal patterns, and have extended this concept to cylindrical and conical surfaces. This paper is structured as follow. In section 2 the split main lobe problem of a plane surface is presented and overcome by introducing surface current theory. Section 3 presents both a conical conformal antenna and a cylindrical conformal antenna. In section 4 a spiral circularly polarized antenna is proposed. The final conclusions in section 5 discuss the main work and significance.

2. Split Main Lobe Problem for Plane Surface Antennas

For scattering of a bound TM modes, the impedance modulation function derived from the holographic interference is

$$\eta_{\text{surf}}(X_t) = j[X + M \text{Re}(\psi_{\text{rad}}\psi_{\text{surf}}^*)] \quad (1)$$

where X is an arbitrary real average impedance value, M is the real modulation depth, and the quantities ψ_{surf} and ψ_{rad} are the phase information of the surface wave travelling upon the impedance surface and the desired radiating plane wave respectively.

To produce a plane wave at 45 degrees in X-Y plane, a small monopole antenna is used as the source. Taking ψ_{surf} and ψ_{rad} in (1), we get the impedance modulation pattern, and the impedance surface is constructed which is shown in Fig. 1.

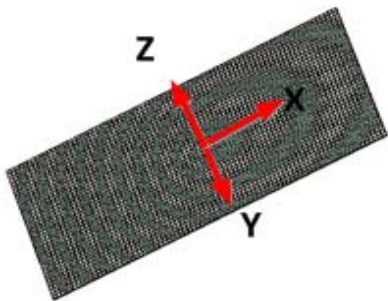


Fig. 1. Simulated model of the antenna

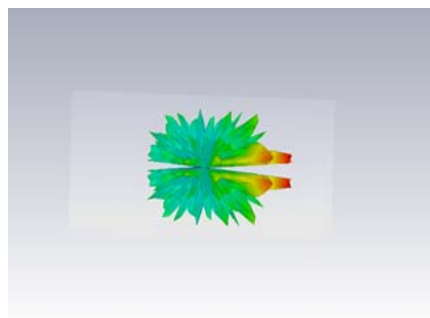


Fig. 2. The 3-D radiation pattern

We are supposed to get the desired radiation pattern when the holographic impedance surface is excited by the corresponding surface wave produced by the monopole, i.e. the main lobe the radiation pattern should be at 45° from Z-axis in X-Y plane. The simulation results displayed in Fig. 2, however, deviate greatly from our expectations. The main lobe appears near the desired direction indeed, but yet splits into two separate parts, resulting in a zero point where there should be the peak point instead.

A reasonable explanation could be that surface current flows in revers directions in two symmetric sections. Consider surface current consists of two orthogonal components, one in X direction and the other Y direction.

Since the impedance surface and the monopole is both symmetric about Z-X plane, the phase difference of surface current in two regions ($y > 0$ and $y < 0$) equals π and the distances between field points in Z-X plane and two corresponding source points on the impedance surface in two regions are identical. As a result, the phi component of the far field radiated by these two regions cancels at Z-X plane, leading to a zero point at the desired main lobe direction. Meanwhile, although the structure is not symmetric in X direction, surface current is also anti-phased in regions $x < 0$ and $x > 0$, which causes radiation cancellation in specific directions as well.

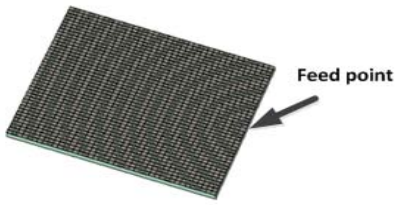


Fig. 3. Simulated model of the first antenna (region: $x < 0$)

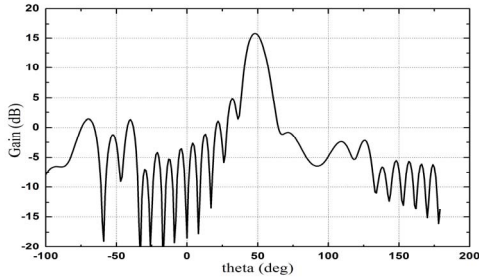


Fig. 4. Simulated radiation pattern at 17 GHz

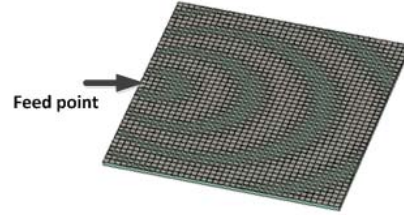


Fig. 5. Simulated model of the second antenna (region: $x > 0$)

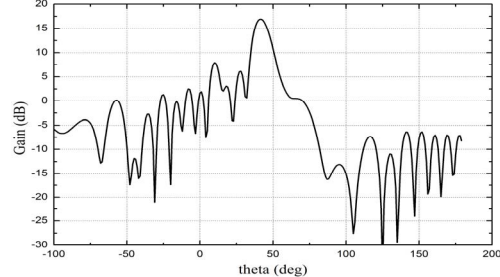


Fig. 6. Simulated radiation pattern at 17 GHz

To demonstrate these assumptions, three different antennas are designed and simulated. As shown in Fig. 3, the first antenna is fed by a monopole located at the left edge of the impedance surface which corresponds to the situation that only region $x < 0$ is active. And Fig. 4 is the corresponding simulation result. Fig. 5 and Fig. 6 are respectively the structure and simulation result of the second antenna of which only region $x > 0$ contributes to the radiation. It can be confirmed from these two antennas that whether surface current flows in X direction or $-X$ direction, the radiation pattern will not be split at the desired angle, which seems to be in conflict with the results shown in Fig. 7 and Fig. 8 where the two antennas are actually placed and excited together.

To prove that the conflict is due to the reverse surface current flowing directions, the third antenna is designed to combine the former two, yet the phase of surface is delayed by π in region $x < 0$ (shown in Fig. 7 and Fig. 8 is the corresponding result). As we can see, the radiation pattern is no longer split and the gain is about 3 dB higher than that of the first or the second one, which is in accordance with our predictions.

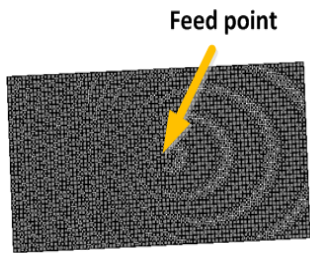


Fig. 7. Simulated model of the third antenna

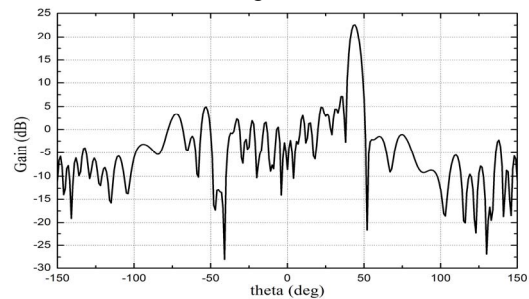


Fig. 8. Simulated radiation pattern at 17 GHz

3. Conical and Cylindrical Surface Conformal Antennas

Conformal antennas for both cylindrical and conical surfaces are designed and present in this section. Unlike the impedance modulation function given by (1), in conformal situations, the coordinate we use in this function should be transformed from Cartesian coordinate to cylindrical coordinate. For a holographic artificial impedance surface antenna in any shape, (1) can be rewritten as

$$\eta_{surf} = j \left[X + M \cos(k_t r - \vec{k}_0 \cdot \vec{r}) \right] \quad (2)$$

where k_t is the surface wave vector, \vec{k}_0 is the desired radiation wave vector, \vec{r} is the three-dimensional

position vector of artificial impedance surface, and r is the distance between the surface-wave source point and the field point corresponding to \vec{r} . In cylindrical coordinate, $\vec{k}_0 \cdot \vec{r}$ can be written as follows:

$$\begin{aligned} \vec{k}_0 \cdot \vec{r} = & k_x \rho \frac{r_c}{\sqrt{r_c^2 + h^2}} \cos \varphi + k_y \rho \frac{r_c}{\sqrt{r_c^2 + h^2}} \sin \varphi \\ & + k_z \rho \frac{h}{\sqrt{r_c^2 + h^2}} \end{aligned} \quad (3)$$

where k_x , k_y and k_z are the three components of radiation wave vector, h is the height of the cone, and r_c is bottom radius.

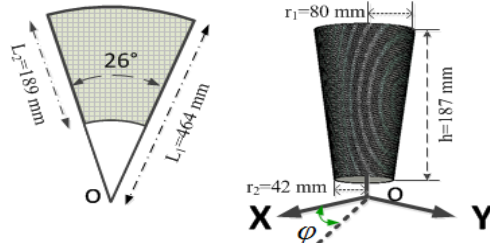


Fig. 9. The layout of the artificial impedance surface. Left: the planar artificial impedance surface. Right: the conical artificial impedance surface.

Take (3) into (2), and the modulated surface impedance is determined. The two impedance surface antennas are fed by a monopole antenna, and the conical conformal antennas simulation results are respectively shown in Fig. 9 and Fig. 10 from which we can see surface wave travels along the conical and cylindrical surfaces and produces radiation wave beams at the desired angles while good VSWR and gain is also achieved.

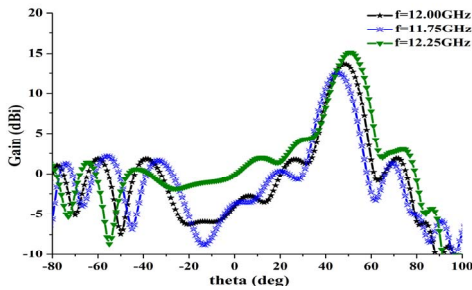


Fig. 10. Radiation pattern in X-Y plane. A simple vertical dipole on the conical surface is used as a feeder. Simulated E-plane radiation patterns for various frequencies at 11.75 GHz, 12 GHz and 12.25 GHz. Side lobe levels are -10.4 dB, -11.8 dB and -12.1 dB.

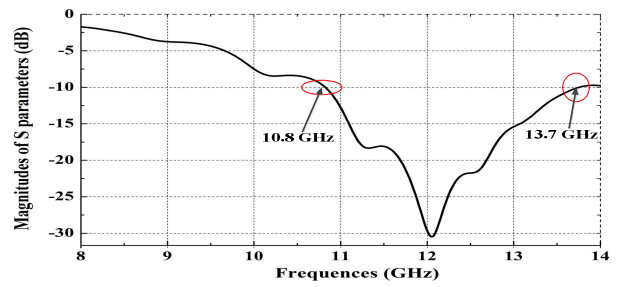


Fig. 11. Simulated reflection coefficient. Magnitudes of S parameters are under -10 dB between 10.8 GHz and 13.7 GHz.

4. Spiral Circularly-Polarized Antenna

Spiral circularly polarized artificial impedance surface antennas are designed by using the holographic technique [4]. We consider a circular surface which possesses an Archimedean spiral reactance sinusoidally modulated along the radial direction. The following expression is the analytical description of such a surface

$$\eta_{surf}(\rho, \varphi) = j[X + M \cos(k_t \rho - \varphi)] \quad (4)$$

where (ρ, φ) is a position on the impedance surface in the X-Y plane. The modulation periodicity along each ray is equal to λ_{sw} , and the difference between the interception with the spiral of two rays separated by 90° is $\lambda_{sw}/4$. Any pair of elemental sectors separated by 90° gives rise at broadside to orthogonal and quadrature-phased components respectively.

As an example, the antenna is realized on substrate Taconic RF-60, with a dielectric constant of 6.15 and thickness of 1.27mm. Method mentioned above is used to obtain the relation between gap size and η_{surf} . For gaps ranging from 1 mm to 0.2 mm, the effective impedance varied from 248.5j to 432.9j ohms at 12.5 GHz. The holographic antenna aperture is 243 mm \times 243 mm shown in Fig.1. A vertical probe is fed by a coaxial to launch a TM_0 surface wave. A slotted circular top hat is used to perform impedance matching and to increase the efficiency of the feeder as a surface wave launcher. Some Simulated results are shown in Fig. 13 ~ Fig.15.



Fig. 12. Simulated model of the antenna

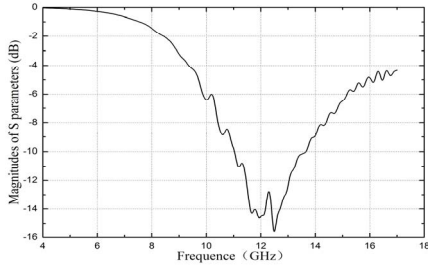


Fig. 13. Simulated reflection coefficient. S_{11} parameter is under -10dB between 10.1 GHz and 13.6 GHz.

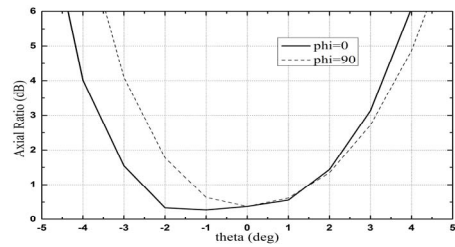


Fig. 14. Simulated axial ratio

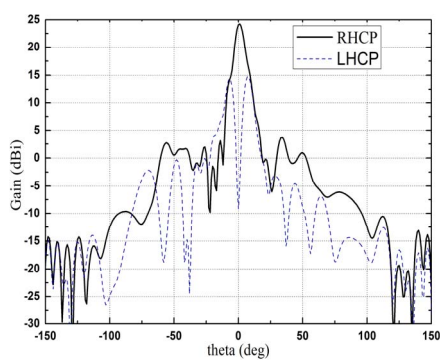
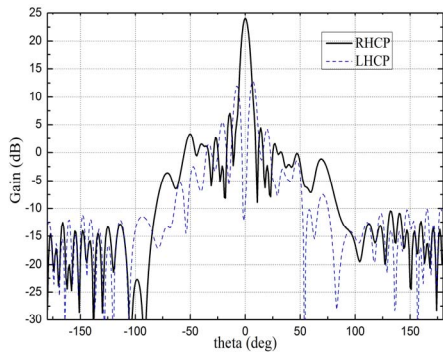


Fig. 15. Simulated radiation pattern. Corresponds to $\phi=0$ and $\phi=90$ respectively

5. Conclusion

In this paper, the split main lobe problem, conformal and circularly-polarized applications of artificial modulated impedance surface antennas are discussed. Simulation models of these antennas are presented as well as the corresponding simulation results. Analyses in this paper have shown good promises of this kind of antennas in both conformal and polarization-controlling applications.

6. Reference

1. A. Oliner and A. hessel, "Guided waves on sinusoidally-modulated reactance surface," IRE Trans. Antennas Propag., Vol. 7, no. 5, pp.201-208, Dec. 1959.
2. D. Sievenpiper, J. Colburn, B. Fong, J. Ottusch, and J. Visher, "Holographic artificial impedance surfaces for conformal antennas," presented at the IEEE Antennas and Propagation Symposium Digest, Washington DC, Jul. 5, 2005.
3. J. Colburn, D. Sievenpiper, B. Fong, J. Ottusch, and P. Herz, "Advances in artificial impedance surface conformal antennas," in IEEE Antennas and Propagation Symposium Digest, Washington DC, Jun. 9, 2007, pp. 3820-3823.
4. G. Minatti, M. Casaletti, F. Caminita, P. De Vita, S. Maci. "Planar antennas based on surface-to-leaky wave transformation." In Proceedings of the 5th European Conference on Antennas and Propagation (EUCAP), pp. 1915-1918. 2011.